JOC The Journal of Organic Chemistry

Article

pubs.acs.org/joc

Hückel and Möbius Bond-Shifting Routes to Configuration Change in Dehydro[4*n*+2]annulenes

Mitchell V. Santander,[†] Michael B. Pastor,[†] Jordan N. Nelson,[†] Claire Castro,*[,†] and William L. Karney*[,†,‡]

[†]Department of Chemistry and [‡]Department of Environmental Science, University of San Francisco, 2130 Fulton Street, San Francisco, California 94117, United States

Supporting Information

ABSTRACT: Computational investigation of the potential energy surfaces of dehydro[10]- and dehydro[14]annulenes revealed that mechanisms involving Hückel and Möbius π-bond shifting can explain the observed or proposed configuration change reactions. Unlike the case of annulenes, in which bond-shift midpoints correspond to transition states, for transformations of dehydroannulenes with Δtrans = 0, "hidden" Hückel bond shifts occur on the side of an energy hill, on the way to a cumulenic, purely conformational transition state. For example, interconversion between CTCCTC-dehydro[14]annulene (**1a**) and CCTCTC-dehydro[14]annulene (**2a**) has a CCSD(T)/cc-pVDZ//BHLYP/6-31G* barrier of 18.7 kcal/mol, consistent with experimental observations, and proceeds via a conformational transition state, with Hückel π-bond shifts occurring both before and after the transition state. However, when Δtrans = 1, a true Möbius π-bond shift transition state was located. The isomerization of CCTC-dehydro[10]annulene (**10**) to CCCC-dehydro[10]annulene (**11**) occurs by an initial "hidden" Hückel bond shift, followed by passage through a Möbius bond-shift transition state to **11**, with an overall barrier of 29.8 kcal/mol at the CASPT2(12,12)/cc-pVDZ//(U)BHLYP/6-31G* level of theory. This is the lowest energy pathway between **10** and **11**, in contrast to a cyclization/ring-opening route via a bicyclic allene described in previous reports.

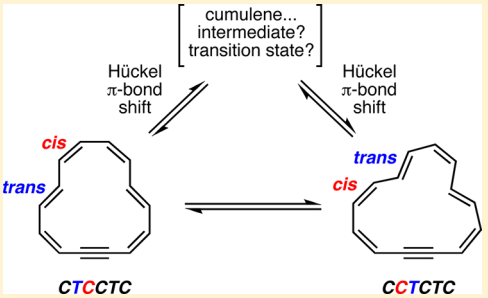

INTRODUCTION

The Möbius−Hückel concept as developed by Zimmerman provides a useful tool for qualitatively determining whether a pericyclic reaction pathway is "allowed" or "forbidden".[1] In short, reactions involving 4*n*+2 electrons are allowed if the relevant orbital basis comprises a Hückel array (0 or an even number of sign inversions) and forbidden if the orbital basis comprises a Möbius array (odd number of sign inversions). Conversely, for reactions involving 4*n* electrons, allowed pathways are characterized by a Möbius array and forbidden routes by a Hückel array. Whereas such topological analysis enables one to assess allowed and forbidden pathways, there exist cases for which *only* a forbidden route will connect reactants to products. Configuration changes in certain annulenes and dehydroannulenes fall into this category, but consideration of Hückel and Möbius topology still proves critical in thinking about the mechanism.[2,3]

Several known examples of thermal cis−trans isomerization in annulenes[4,5] have been explained by π-bond shifting, in particular via Möbius conformations.[3,5] The π-bond shift rule enables one to determine the topology required to effect a given transformation.[2] With an even higher carbon to hydrogen ratio than in annulenes, dehydroannulenes are of interest as potential precursors to carbon-rich materials.[6] Following our recent computational study of the structures, energetics, and interconversions of dehydro[12]annulene isomers,[7] we here report density functional, coupled cluster, and CASPT2 calculations on known and proposed configuration change reactions in two [4*n*+2] systems—dehydro[14]- and dehydro[10]annulenes.

BACKGROUND

Despite their position between annulenes and systems with much higher carbon to hydrogen ratios, medium-sized monodehydroannulenes (C_nH_{n-2} with n = 10, 12, 14, 16) have proven difficult to synthesize and characterize.[8,9] Although substituted monodehydro[10]annulenes have been invoked as possible intermediates in dehydro Diels−Alder reactions[10] (vide infra), the synthesis of the parent system has yet to be realized. More recently, Christl and Hopf showed that dehydro[12]annulene isomers have not been prepared,[11] despite prior reports to the contrary.[12] There are no reports for the synthesis of monodehydro[16]annulene. Thus, the work of Sondhemier et al. on dehydro[14]annulene stands out as the sole successful synthesis of a monodehydro medium-sized annulene.[8,13] A more complete understanding of the reactivity

Special Issue: Howard Zimmerman Memorial Issue

Received: September 20, 2012
Published: October 29, 2012

of these elusive species may help in their future identification as well as help in predicting the reactivity of substituted analogues.

Sondheimer and co-workers described the configurational isomerism of monodehydro[14]annulene.[8,13] Two different isomers were observed by NMR—a "stable" and an "unstable" isomer—both with a 5:1 ratio of outer to inner hydrogens. The unstable isomer converted to the stable configuration on standing in ether solution at room temperature for 24 h.[13] Whereas the two isomers were ultimately assigned to structures **1** and **2** (Scheme 1),[8] Sondheimer et al. could not confidently

Scheme 1

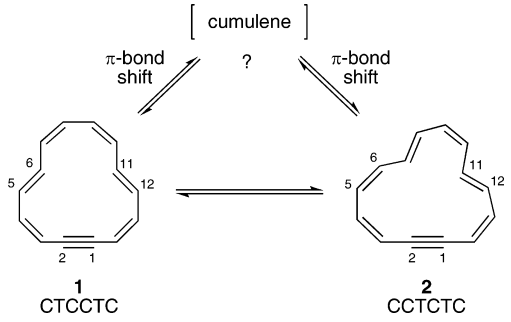

state which was the more stable.[14] No mechanism was proposed for the interconversion of **1** and **2**. This observed reaction thus represents an excellent opportunity to test the scope of the π-bond shift rule in dehydro[4*n*+2]annulenes and to determine whether cumulenes act as intermediates or transition states in such processes.

More recently, configuration changes in dehydro[10]annulene derivatives have been invoked to explain the observation of rearranged products of dehydro Diels–Alder reactions.[15] For example, Saá and co-workers found that phenylpropiolamides **3** afford products **4** (expected) and **5** (unexpected), and Echavarren et al. reported that arylpropinones **6** yield the corresponding benzo[*b*]fluorenones **7** (expected) and benzo[*a*]fluorenones **8** (unexpected) (Scheme 2).[10]

Scheme 2

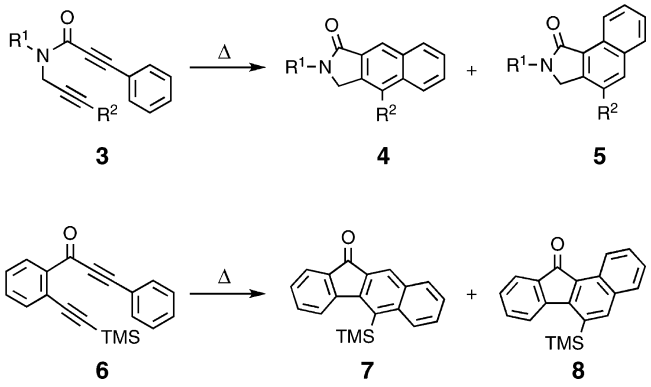

The reactions in Scheme 2 proceed by initial formation of a cyclic allene (specifically a 1,2,4-cyclohexatriene), which can undergo ring opening to give a dehydro[10]annulene. Subsequent cis–trans isomerization of the dehydro[10]annulene, followed by electrocyclization, yields the rearranged skeleton. The groups of Saá[10a] and Schreiner[16] have reported relevant calculations—Saá on the reaction of **3** to give **4** and **5** and Navarro-Vázquez and Schreiner on possible processes in the $C_{10}H_8$ core. In an attempt to explain the formation of observed products **4** and **5** (Scheme 1), Saá computed a one-step mechanism for the key isomerization of **12** to **13** (R^1 = CH_3, R^2 = H), with a B3LYP/6-31G* barrier of 18–20 kcal/mol.[10a]

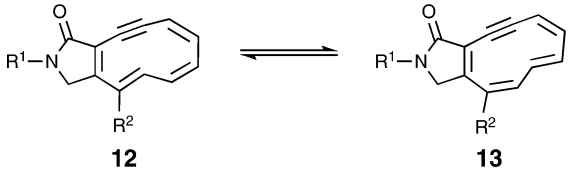

Navarro-Vázquez and Schreiner computationally located a similar one-step mechanism for the $C_{10}H_8$ core reaction **10** → **10′** (Scheme 3) with a 13.5 kcal/mol barrier (CCSD(T)/cc-

Scheme 3

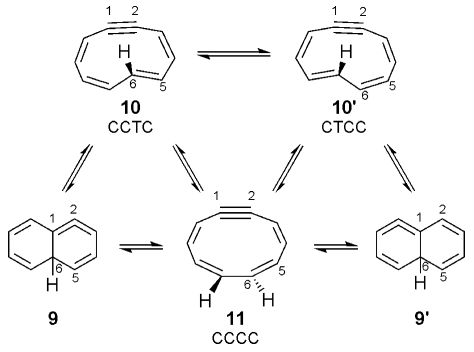

pVDZ//B3LYP/6-31G*) and a cumulenic transition state. In addition, they considered the intriguing possibility that an all-cis (CCCC) dehydro[10]annulene (**11**) might be involved,[16] as originally suggested by Echavarren for the reaction of **6**,[10d] and computed a variety of mechanisms connecting **10** and **11**. At the CCSD(T) level, a cyclization/ring-opening pathway via cyclic allene **9** (Scheme 3) was predicted to have a somewhat lower barrier ($E_a \approx 37$ kcal/mol) than an intriguing but high-energy one-step route via a delocalized Möbius transition state ($E_a \approx 46$ kcal/mol).[16] Using multiconfigurational perturbation theory, the Möbius transition state was computed to be ca. 37 kcal/mol higher than **10**. Although Navarro-Vázquez and Schreiner presented a detailed picture of the $C_{10}H_8$ PES, multiconfigurational results were presented only for selected species, making it difficult to compare the different possible mechanistic pathways. Revisiting the dehydro[10]annulene hypersurface with multiconfigurational methods, to compare closed-shell and singlet-diradical pathways on an equal footing, seems warranted. In addition, at the time of the Navarro-Vázquez and Schreiner study, the bond-shift rule had not yet been developed, which might have aided in locating likely transition states. This rule states that annulene configuration change reactions with Δtrans = 0, 2 can occur by Hückel-topology π-bond shifting, whereas reactions with Δtrans = 1 *require* a Möbius π-bond shifting step.[2,3] The bond-shift rule emerges from the fact that Möbius-topology annulenes have an odd number of transoid units (CCCC units with dihedral angle ω such that $90° < |\omega| \leq 180°$), whereas Hückel topology is characterized by an even number of transoid units.

Dehydro[10]annulenes lie at the heart of likely mechanisms connecting the isomeric isonaphthalenes **9** and **9′**. Given that

dx.doi.org/10.1021/jo302072p | J. Org. Chem. 2013, 78, 2033–2039

alkynes (relative to cumulenes) are generally the more stable forms of dehydroannulenes, elucidation of bond-shifting pathways for cis/trans isomerization in these systems requires first the recognition that two bond-shift steps are needed to get from one alkyne isomer to another—one π-bond shift to produce a cumulene and a second π-bond shift to regenerate an alkyne. Even though two π-bond shifts would be necessary, the overall Δtrans value for the process will determine if one of those π-bond shifts needs to be Möbius. For example, previous work on the conversion of CTCTC- to CCTCC-dehydro[12]-annulene showed that, because Δtrans = 1, one of the two bond-shift steps must proceed with Möbius topology and the other bond-shift step must go with Hückel topology (Scheme 4). Thus, the bond-shift rule provides a useful tool for analyzing conversions in dehydroannulenes as well as annulenes.

Scheme 4

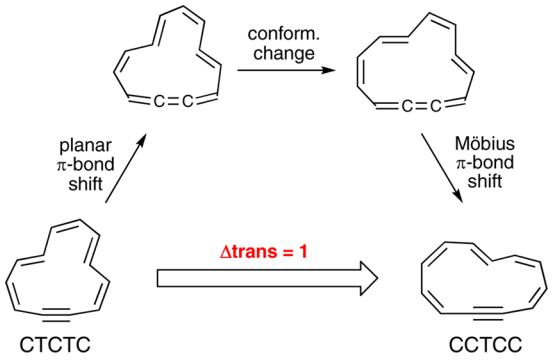

Here we report computational results on π-bond-shifting mechanisms for configuration changes in both dehydro[14]- and dehydro[10]annulenes. These results reveal not only that such mechanisms are viable for cis/trans isomerization in dehydro[14]annulene but also that the computed barrier for interconversion of dehydro[10]annulenes **10** and **11** is much lower than that predicted by previous calculations.

COMPUTATIONAL METHODS

Geometry optimizations and vibrational analyses were performed using the BHandHLYP method (here abbreviated BHLYP),[17] in conjunction with the 6-31G* basis set. This method has been shown to afford geometries that reasonably reflect the degree of delocalization in annulenes.[18] Systems with diradical character, such as the delocalized Möbius dehydro[10]annulenes, were computed with a broken spin symmetry, unrestricted wave function. Transition states were verified by the presence of exactly one imaginary vibrational frequency. Zero-point energies (ZPEs) were obtained from the unscaled vibrational frequencies. Intrinsic reaction coordinate (IRC) calculations were performed on key transition states at the (U)BHLYP/6-31G* level using force constants obtained from the preceding vibrational analyses.

To account for dynamic electron correlation, single-point energies for all $C_{10}H_8$ species were computed at the CASPT2(12,12)/cc-pVDZ level[19] at the (U)BHLYP/6-31G* geometries. All $C_{10}H_8$ species were computed using a 12-electron, 12-orbital active space. For dehydro[10]annulene isomers **10** and **11**, the active space consisted of all π and π* MOs, including the "in-plane" π MOs of the acetylene moiety. For the bicyclic allene and associated transition states, the active space included the σ/σ* pair for the bridging bond, plus 10 π/π* MOs. An IPEA (ionization potential−electron affinity) shift of 0.25 was used for all CASPT2 calculations. Single-point energies for all $C_{14}H_{12}$ species were computed at the CCSD(T)/cc-pVDZ level on the BHLYP geometries. Relative energies are corrected for differences in the (U)BHLYP/6-31G* ZPEs. Nucleus-independent chemical shifts (NICS)[20] were computed at ring centers of selected species at the GIAO-B3LYP/6-31G* level using the BHLYP geometries.

Density functional and coupled cluster calculations were performed with Gaussian 03 and Gaussian 09.[21] CASPT2 calculations were performed with MOLPRO.[22] Vibrations and molecular orbitals were visualized using Molden.[23]

RESULTS AND DISCUSSION

Dehydro[14]annulene. The BHLYP/6-31G* optimized structures of the two lowest energy conformers of **1** and **2** are shown in Figure 1. Additional conformers of these and other

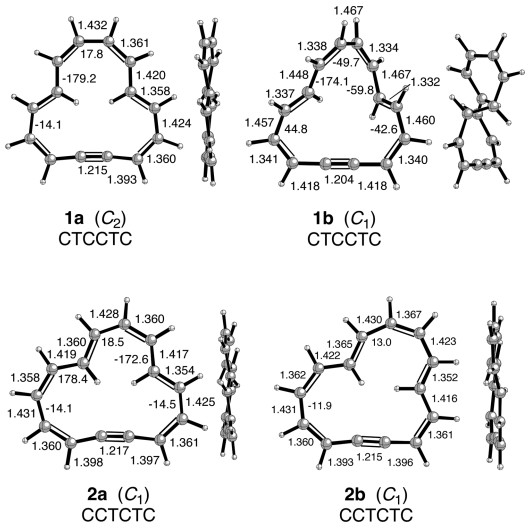

Figure 1. BHLYP/6-31G* optimized structures and edge views of low-energy conformers of CTCCTC- and CCTCTC-dehydro[14]-annulenes **1** and **2**. Selected C−C distances (Å) and CCCC dihedral angles centered on single bonds (deg) are shown.

configurations[24] can be found in the Supporting Information. The C−C bond lengths indicate that, at the BHLYP level, all the conformers located are alkynes rather than cumulenes (1,2,3-butatrienes). All attempts to find cumulene minima (i.e., by choice of initial bond lengths) resulted in structures optimizing to alkynes. All structures show significant bond-length alternation, **1b** more than the others.[25] It is worth noting that conformer **1b** has Möbius topology, by virtue of its possessing an odd number of transoid units. Several other conformers of **1** and **2** have Möbius topology, and their structures are provided in the Supporting Information.

The relative energies of dehydro[14]annulene isomers are provided in Table 1. Each configuration has one conformation that is much more stable than the others; **1a** is 6.4 kcal/mol lower than the next most stable conformer of **1** (**1b**), and **2a** is 5.4 kcal/mol more stable than the next lowest conformer of **2** (**2b**). (See the Supporting Information for structures of other conformers.) In addition, **1a** is computed to be 1.0 kcal/mol more stable than **2a**. The energies of **1a** and **2a** support Sondheimer's experimental results, though the barrier to their interconversion is lacking.

Applying the bond-shift rule to the interconversion of **1a** (CTCCTC) and **2a** (CCTCTC), with Δtrans = 0, gives the conclusion that the two bond shifts required either must both have Hückel topology or must both have Möbius topology. A reasonable mechanism would involve a planar π-bond shift from alkyne **1a** to a corresponding cumulene (with CTCTC

dx.doi.org/10.1021/jo302072p | J. Org. Chem. 2013, 78, 2033−2039

Table 1. Relative Energies (kcal/mol) of Dehydro[14]annulene Stationary Points

compd	config[a]	sym	topol[b]	NI[c]	rel E BHLYP[d]	rel E CCSD(T)[e]
1a	CTCCTC	C_2	Hückel	0	0.0	0.0
1b	CTCCTC	C_1	Möbius	0	10.7	6.4
1c	CTCCTC	C_1	Hückel	0	8.7	7.3
1d	CTCCTC	C_2	Hückel	0	13.7	8.3
1e	CTCCTC	C_1	Möbius	0	15.4	10.1
1f	CTCCTC	C_2	Möbius	0	15.9	11.0
2a	CCTCTC	C_1	Hückel	0	1.5	1.0
2b	CCTCTC	C_1	Hückel	0	6.8	6.4
2c	CCTCTC	C_1	Möbius	0	13.4	8.8
2d	CCTCTC	C_1	Möbius	0	16.1	11.0
2e	CCTCTC	C_1	Hückel	0	15.9	12.2
2f	CCTCTC	C_1	Hückel	0	15.8	14.6
TS1	CTCTC	C_1	Möbius	1	21.9	18.7

[a]Cis–trans configuration: C, cis; T, trans. Six letters indicate an alkyne. Five letters indicate a cumulene. [b]Topology: even number of transoid units, Hückel; odd number of transoid units, Möbius. [c]Number of imaginary frequencies. [d]BHLYP/6-31G*. [e]CCSD(T)/cc-pVDZ//BHLYP/6-31G*.

configuration), then a conformation change, and a second Hückel-topology bond shift to give alkyne **2a**, as shown:

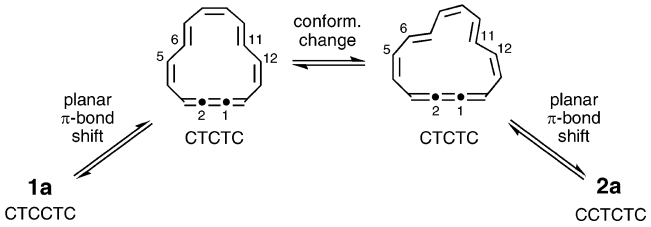

With this hypothesis in mind, exploration of the potential surface revealed a single transition state, **TS1**, connecting **1a** and **2a**. The structure of **TS1** is shown in Figure 2. Transition

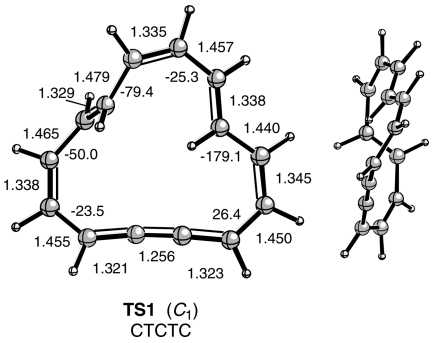

Figure 2. BHLYP/6-31G* optimized structure and edge view of transition state **TS1**, which connects dehydro[14]annulene minima **1a** and **2a**. With three transoid units, **TS1** has nominal Möbius topology. Selected C–C distances (Å) and CCCC dihedral angles centered on single bonds (deg) are shown.

state **TS1** has a cumulenic structure and nominal Möbius topology. One of the trans C=C bonds (C6–C7) is rotated such that the π overlap with the rest of the ring is poor.

Figure 3 shows the results of BHLYP/6-31G* intrinsic reaction coordinate (IRC) analysis for the one-step mechanism between **1a** and **2a**. The two bond-shift midpoints, indicated by dotted lines, are sharply defined, as evidenced by the tight

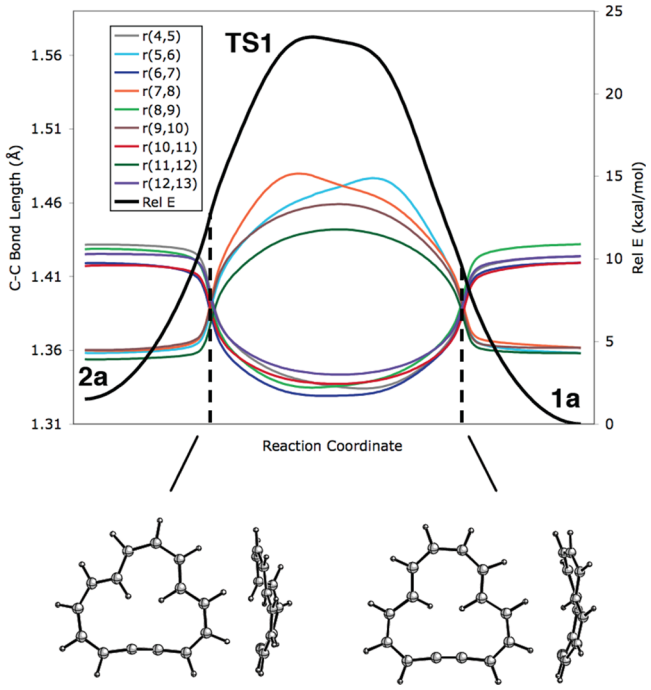

Figure 3. BHLYP/6-31G* intrinsic reaction coordinate analysis from **TS1** to CCTCTC-dehydro[14]annulene (**2a**, left side) and CTCCTC-dehydro[14]annulene (**1a**, right side), depicting relative energies and selected C–C bond lengths. The atom numbering is as in Scheme 1. Dotted lines correspond to midpoints of bond shifting, with corresponding structures and edge views shown below. In either direction, the reaction consists of a Hückel π-bond shift, then conformation change, followed by a second Hückel π-bond shift.

intersection of the bond-length curves, and they occur well away from the transition state. From **2a**, the bond-shift midpoint occurs at a point 10.2 kcal/mol above **2a** and 8.7 kcal/mol below **TS1**. The other bond-shift midpoint lies 7.8 kcal/mol above **1a** and 12.6 kcal/mol below **TS1**. The bond-shift midpoints flanking **TS1** occur relatively high up on the energy curve. Despite this, the geometries at the bond-shift midpoints possess even numbers of transoid units and therefore have Hückel topology. Thus, the sequence of Hückel π-bond shift, conformation change, and Hückel π-bond shift connects **1a** and **2a** via a single transition state.

Dehydro[10]annulene. Figure 4 depicts the BHLYP/6-31G* optimized geometries of the two primary isomers of dehydro[10]annulene, **10** and **11**, and Table 2 shows their relative energies. These geometries are very similar to those previously reported by Schreiner at different levels of theory.[16] The CCTC isomer **10** is nearly planar, with one hydrogen pointing into the center of the ring, whereas the CCCC isomer **11** is much less planar. At the BHLYP level, **11**, with only one transoid unit (C5–C6–C7–C8 dihedral angle of 116°), has Möbius topology.

In agreement with Navarro-Vázquez and Schreiner,[16] we find that automerization of **10** can occur via the transition state **TS2**, which has a pronounced cumulenic structure and nominal Möbius topology (Figure 4). Because of our interest in also computing the barrier for **10** → **11** (Δtrans = 1, open shell) and comparing all energies at a single level of theory, it was important to choose a method that could reliably compute both open- and closed-shell species. At the CASPT2 level, the barrier for automerization of **10** is 14.7 kcal/mol (Table 2), in

dx.doi.org/10.1021/jo302072p | J. Org. Chem. 2013, 78, 2033–2039

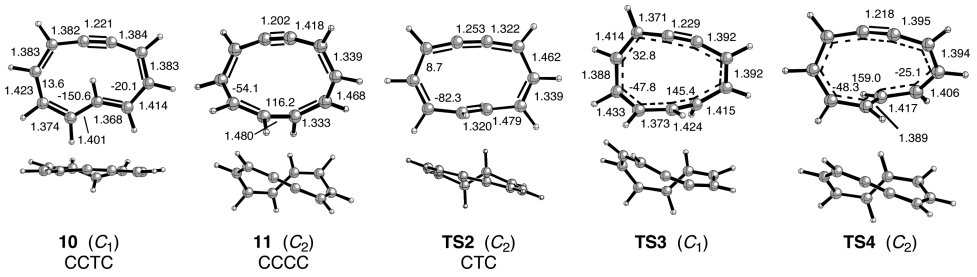

Figure 4. (U)BHLYP/6-31G* optimized structures of dehydro[10]annulene minima and transition states. Edge views also shown. C−C distances (Å) and selected CCCC dihedral angles centered on single bonds (deg) are shown.

Table 2. Relative Energies (kcal/mol) of $C_{10}H_8$ Stationary Points

					rel E	
compd	config[a]	sym	topol[b]	NI	BHLYP[d]	CASPT2[e]
9		C_1		0	10.4	1.1
10	CCTC	C_1	Hückel	0	0.0	0.0
11	CCCC	C_2	Möbius	0	11.1	10.6
TS2	CTC	C_2	Möbius	1	16.2	14.7
TS3		C_1	Möbius	1	32.4[f]	39.0
TS4		C_2	Möbius	1	24.0[g]	29.8
TS5		C_1		1	24.8	14.7
TS6		C_1		1	45.9	36.1

[a]Cis−trans configuration. Four letters indicate an alkyne. Three letters indicate a cumulene. [b]Topology: even number of transoid units, Hückel; odd number of transoid units, Möbius. [c]Number of imaginary frequencies. [d](U)BHLYP/6-31G*. Unrestricted calculations were used for **TS3** and **TS4**. [e]CASPT2(12,12)/cc-pVDZ//(U)BHLYP/6-31G*, using an IPEA shift of 0.25. [f]$\langle S^2\rangle$ = 1.30. [g]$\langle S^2\rangle$ = 1.33.

reasonable accord with Navarro-Vázquez and Schreiner's CCSD(T) value of 13.5 kcal/mol.[16] This mechanism is also consistent with that found computationally by Saá et al. for the reaction of **12** to **13**.[10a]

Automerization of **10** has Δtrans = 0 and therefore should involve two Hückel-topology bond shifts. Indeed, analogous to the case of dehydro[14]annulene described above, BHLYP/6-31G* IRC analysis confirms that the overall automerization pathway thus consists of a Hückel-topology bond shift to a cumulenic structure, followed by conformation change (rotation of the trans C═C bond) passing through the transition state **TS2**, and finally a second Hückel-topology bond shift. In accord with the bond-shift rule for a transformation with Δtrans = 0, neither bond shift has Möbius topology. The bond-shift midpoints are only 2.2 kcal/mol above **10** in energy.

More intriguing is the process connecting the CCTC and CCCC isomers of dehydro[10]annulene, **10** and **11**. In contrast to the "hidden" bond shifts in the automerization described above, the conversion of CCTC- to CCCC-dehydro[10]annulene can occur via a true bond-shift transition state. For this overall process, Δtrans = 1; thus, one of the two required π-bond shifts must have Möbius topology. Navarro-Vázquez and Schreiner indeed located an unsymmetrical Möbius bond-shift transition state (**TS3**, Figure 4) linking **10** and **11**. However, the C_2 symmetry of **11**, along with the C_2 symmetry and Möbius topology of the cumulenic transition state **TS2**, suggests that a different Möbius bond-shift transition state might also connect **10** and **11**. Specifically, **TS2** could serve as a starting point for locating a Möbius π-bond shift toward **11**. Indeed, at the UBHLYP/6-31G* level, the C_2-symmetric structure **TS4** was located and found to perform this role. **TS4** is computed to be significantly more delocalized than **TS3** (Δr = 0.028 Å for **TS4** vs 0.060 Å for **TS3**),[26] due to generally smaller torsional angles in **TS4** (Figure 4).

The energetics for the different routes connecting **10** and **11** are summarized in Figure 5 and Table 2. At the CASPT2 level,

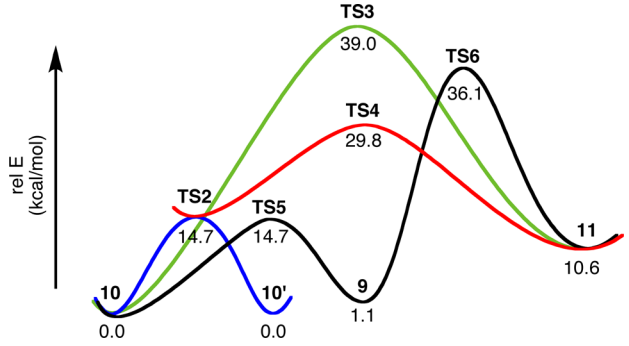

Figure 5. CASPT2(12,12)/cc-pVDZ//(U)BHLYP/6-31G* energy diagram (kcal/mol) showing the automerization and interconversion of dehydro[10]annulene isomers. Conversion of **10** to **11** does not have to pass through **TS2**. The structures of **9**, **TS5**, and **TS6** are given in the Supporting Information.

the barrier for **10** → **11** via **TS4** is computed to be 29.8 kcal/mol. At the same level of theory, this route is predicted to be fully 9 kcal/mol lower in activation energy than that via **TS3** and 6.3 kcal/mol lower than the cyclization/ring-opening pathway via bicyclic allene **9** (the lowest energy pathway found by Navarro-Vázquez and Schreiner). Thus, the Möbius bond-shifting mechanism through **TS4** is the lowest energy path between **10** and **11**.

The degree of diradical character in **TS4** is perhaps not as large as one would expect for a delocalized Möbius [10]-annulene. Of the two nonbonding MOs depicted in Figure 6, the *b* orbital has an occupation of 1.42e, and the *a* orbital an occupation of 0.58e, from CASSCF calculations.

The lowest-energy route for **10** → **11** is somewhat analogous to bond shifting in cyclooctatetraene (COT), in which ring inversion occurs via a D_{4h} symmetric transition state and π-bond shifting via a D_{8h} transition state.[27] Isomer **10** rises first in the direction of the conformational transition state **TS2**, but without necessarily passing through **TS2** the molecule then ascends along a different coordinate to the C_2-symmetric bond-shift transition state **TS4**. No intermediate occurs on this pathway connecting **10** and **11**.

The results of IRC calculations and bond-length analysis similar to that described for the dehydro[14]annulene are shown in Figure 7. From the bond-shift transition state **TS4**,

dx.doi.org/10.1021/jo302072p | J. Org. Chem. 2013, 78, 2033−2039

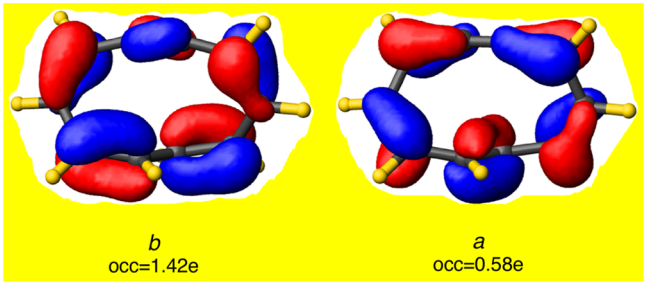

Figure 6. The two nonbonding MOs (NBMOs) of Möbius bond-shift transition state **TS4**. Occupation numbers are from CASSCF(12,12)/cc-pVDZ calculations on the UBHLYP/6-31G* geometry.

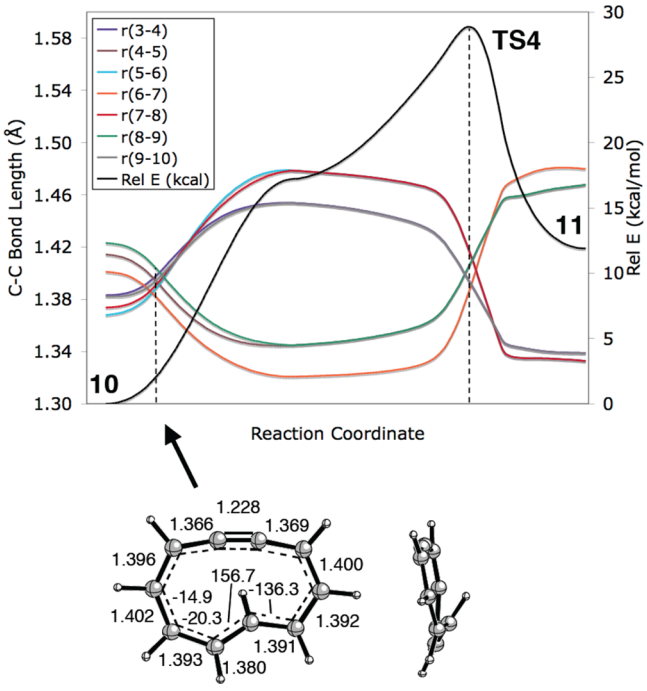

Figure 7. UBHLYP/6-31G* intrinsic reaction coordinate analysis from **TS4** to dehydro[10]annulene isomers **10** and **11**, depicting relative energy (kcal/mol) and selected C−C bond lengths. The attom numbering is as in Scheme 3. Dotted lines correspond to approximate midpoints of bond shifting. The structure of the Hückel-topology bond-shift midpoint closest to **10** is shown below the plot, with C−C distances (Å) and selected CCCC dihedral angles (deg) given.

moving to the right represents a steep descent directly to the strongly bond-alternating alkyne structure **11**. Moving left from **TS4**, the system quickly achieves a cumulenic structure, as evident from the large difference between long and short C−C bonds and the fact that the C3−C4 and C9−C10 bonds are long at that point. Rather than passing directly through **TS2**, the system must reach a valley ridge inflection point,[28] i.e. a bifurcation on the potential energy surface, where the molecule changes from C_2 to C_1 symmetry and descends the rest of the way—including a hidden bond shift—to one of the enantiomers of **10**.

CONCLUSIONS

Just as it does for annulenes, π-bond shifting provides mechanistic pathways for thermal configuration change in dehydroannulenes. The preference for alkyne forms of dehydroannulenes necessitates two bond-shift steps. In analogy with bond shifting in cyclooctatetraene, the Möbius bond-shift transition state **TS4** in dehydro[10]annulene (CCTC to CCCC conversion, Δtrans = 1), which has singlet diradical character, is the bond-equalized form of the cumulenic transition state **TS2** for bond-shift automerization of the CCTC isomer (Δtrans = 0). With CASPT2(12,12)/cc-pVDZ//(U)BHLYP/6-31G* the barrier for **10** to **11** via **TS4** is 29.8 kcal/mol, which is ca. 6 kcal/mol lower than a previously suggested mechanism connecting these two isomers and involving a bicyclic allene intermediate.

A one-step mechanism for configuration change in dehydro[14]annulene (CTCCTC **1a** to CCTCTC **2a**, Δtrans = 0) was located, with a 18.7 kcal/mol barrier (CCSD(T)/cc-pVDZ//BHLYP/6-31G*) consistent with Sondheimer's observation that **1a** and **2a** interconvert at room temperature in solution. Hidden Hückel π-bond shifts occur both before and after a cumulenic conformational transition state. Though cumulenes play a role in these reactions, they are not intermediates but rather act as transition states, specifically as conformational transition states. The hidden π-bond shifts are perhaps analogous to recently studied concerted carbocation rearrangements, in which σ-bond shifts occur at points along a reaction coordinate distant from the transition state.[29]

The pattern that emerges in dehydro[4*n*+2]annulenes is that "allowed" π-bond shifts can often be hidden, i.e. can occur on the side of an energy hill (adjacent to a cumulenic transition state), whereas "forbidden" π-bond shifts must pass through a true bond-shift transition state. While the π-bond shift rule allows one to determine the necessary topology for a given transformation, it is Zimmerman's Möbius−Hückel concept that enables one to decide whether the necessary bond shifts are "allowed" or "forbidden". In Zimmerman transition states, which involved both π and σ bonds, the allowed pathway was always favored due to its closed-shell nature. Configuration changes in annulenes and dehydroannulenes are unique in that only π electrons are involved in bond shifting. For these systems both "allowed" and "forbidden" pathways are feasible. Nonetheless, understanding whether a reaction is allowed or forbidden enables one to determine if closed-shell or open-shell methods are appropriate.

ASSOCIATED CONTENT

Supporting Information

Tables, figures, and text giving absolute energies and Cartesian coordinates for all stationary points, IRC analysis of transition state **TS2**, details of conformational interconversions of **1** and **2**, and complete citation for ref 21. This material is available free of charge via the Internet at http://pubs.acs.org.

AUTHOR INFORMATION

Corresponding Author

*E-mail: castroc@usfca.edu; karney@usfca.edu.

Notes

The authors declare no competing financial interest.

ACKNOWLEDGMENTS

We thank the National Science Foundation (Grant Nos. CHE-0910971 and CHE-1213425) and the University of San Francisco Faculty Development Fund for supporting this work.

REFERENCES

(1) Zimmerman, H. *Acc. Chem. Res.* **1971**, *4*, 272.

(2) Moll, J. F.; Pemberton, R. P.; Gutierrez, M. G.; Castro, C.; Karney, W. L. *J. Am. Chem. Soc.* **2007**, *129*, 274.
(3) Castro, C.; Karney, W. L. *J. Phys. Org. Chem.* **2012**, *25*, 612.
(4) (a) Oth, J. F. M. *Pure Appl. Chem.* **1971**, *25*, 573. (b) Oth, J. F. M.; Röttele, H.; Schröder, G. *Tetrahedron Lett.* **1970**, 61. (c) Oth, J. F. M.; Gilles, J.-M.; Schröder, G. *Tetrahedron Lett.* **1970**, 67.
(5) Eichberg, M. J.; Houk, K. N.; Lehmann, J.; Leonard, P. W.; Märker, A.; Norton, J. E.; Sawicka, D.; Vollhardt, K. P. C.; Whitener, G. D.; Wolff, S. *Angew. Chem., Int. Ed.* **2007**, *46*, 6894.
(6) Haley, M. M., Tykwinski, R. R., Eds. *Carbon-Rich Compounds: From Molecules to Materials*; Wiley-VCH: Weinheim, Germany, 2006.
(7) Januar, L. A.; Huynh, V.; Wood, T. S.; Castro, C.; Karney, W. L. *J. Org. Chem.* **2011**, *76*, 403.
(8) Sondheimer, F. *Acc. Chem. Res.* **1972**, *5*, 81.
(9) Balaban, A. T.; Banciu, M.; Ciorba, V. *Annulenes, Benzo-, Hetero-, Homo-Derivatives, and their Valence Isomers*; CRC Press: Boca Raton, FL, 1987; Vol. *I*.
(10) (a) Rodríguez, D.; Navarro-Vázquez, A.; Castedo, L.; Domínguez, D.; Saá, C. *J. Am. Chem. Soc.* **2001**, *123*, 9178. (b) Rodríguez, D.; Navarro-Vázquez, A.; Castedo, L.; Domínguez, D.; Saá, C. *J. Org. Chem.* **2003**, *68*, 1938. (c) Rodríguez, D.; Martínez-Esperón, M. F.; Navarro-Vázquez, A.; Castedo, L.; Domínguez, D.; Saá, C. *J. Org. Chem.* **2004**, *69*, 3842. (d) Atienza, C.; Mateo, C.; de Frutos, Ó.; Echavarren, A. M. *Org. Lett.* **2001**, *3*, 153. (e) González-Cantalapiedra, E.; de Frutos, Ó.; Atienza, C.; Mateo, C.; Echavarren, A. *Eur. J. Org. Chem.* **2006**, 1430.
(11) Christl, M.; Hopf, H. *Angew. Chem., Int. Ed.* **2010**, *49*, 492.
(12) (a) Gard, M. N.; Kiesewetter, M. K.; Reiter, R. C.; Stevenson, C. D. *J. Am. Chem. Soc.* **2005**, *127*, 16143. (b) Rose, B. D.; Reiter, R. C.; Stevenson, C. D. *Angew. Chem., Int. Ed.* **2008**, *47*, 8714.
(13) (a) Jackman, L. M.; Sondheimer, F.; Amiel, Y.; Ben-Efraim, D. A.; Gaoni, Y.; Wolovsky, R.; Bothner-By, A. A. *J. Am. Chem. Soc.* **1962**, *84*, 4307. (b) Sondheimer, F.; Calder, I. C.; Elix, J. A.; Gaoni, Y.; Garratt, P. J.; Grohmann, K.; di Maio, G.; Mayer, J.; Sargent, M. V.; Wolovsky, R. *Chem. Soc. Spec. Publ.* **1967**, *No. 21*, 75.
(14) This interpretation constituted a revision of earlier explanations, which assigned both observed species as different conformations of **1**.[13]
(15) For related reviews see: (a) Johnson, R. P. *J. Phys. Org. Chem.* **2010**, *23*, 283−292. (b) Wessig, P.; Müller, G. *Chem. Rev.* **2008**, *108*, 2051. (c) See also: Ajaz, A.; Bradley, A. Z.; Burrell, R. C.; Li, W. H. H.; Daoust, K. J.; Bovee, L. B.; DiRico, K. J.; Johnson, R. P. *J. Org. Chem.* **2011**, *76*, 9320.
(16) Navarro-Vázquez, A.; Schreiner, P. R. *J. Am. Chem. Soc.* **2005**, *127*, 8150.
(17) (a) Becke, A. D. *J. Chem. Phys.* **1992**, *98*, 1372. (b) Miehlich, B.; Savin, A.; Stoll, H.; Preuss, H. *Chem. Phys. Lett.* **1989**, *157*, 200.
(18) (a) Wannere, C. S.; Sattelmeyer, K. W.; Schaefer, H. F.; Schleyer, P. v. R. *Angew. Chem., Int. Ed.* **2004**, *43*, 4200. (b) Castro, C.; Karney, W. L.; Vu, C. M. H.; Burkhardt, S. E.; Valencia, M. A. *J. Org. Chem.* **2005**, *70*, 3602.
(19) (a) Andersson, K.; Malmqvist, P.-Å.; Roos, B. O.; Sadlej, A. J.; Wolinski, K. *J. Phys. Chem.* **1990**, *94*, 5483. (b) Andersson, K.; Malmqvist, P.-Å.; Roos, B. O. *J. Chem. Phys.* **1992**, *96*, 1218. (c) Celani, P.; Werner, H.-J. *J. Chem. Phys.* **2000**, *112*, 5546.
(20) Schleyer, P. v. R.; Maerker, C.; Dransfeld, A.; Jiao, H.; Hommes, N. J. R. v. E. *J. Am. Chem. Soc.* **1996**, *118*, 6317.
(21) (a) Frisch, M. J. et al. *Gaussian 03, Revision D.01*; Gaussian, Inc., Wallingford, CT, 2004. (b) Frisch, M. J. et al. *Gaussian 09, Revision A.02*; Gaussian, Inc., Wallingford, CT, 2009.
(22) Werner, H.-J.; Knowles, P. J.; Knizia, G.; Manby, F. R.; Schütz, M. et al. *MOLPRO, version 2010.1, a package of ab initio programs*; see http://www.molpro.net.
(23) Schaftenaar, G.; Noordik, J. H. *J. Comput.-Aided Mol. Design* **2000**, *14*, 123.
(24) Other configurations considered included CCTTCC, CCCCTC, and CCCCCC. The only conformer located for the CCTTCC isomer (**14**) had C_2 symmetry and a nearly planar geometry and was computed to be 6.2 kcal/mol less stable than **1a**. Species **14** was ruled out on energetic grounds. The two conformers located for the CCCCTC configuration (**15a,b**) were computed to be 3.0 and 4.6 kcal/mol less stable than **1a**. These two species were not considered to be responsible for Sondheimer's observed NMR spectra, on the grounds that they did not possess the required two internal hydrogens necessary to be consistent with the observed NMR spectra. The only conformer located for the CCCCCC isomer (**16**) was predicted to be 14.9 kcal/mol less stable than **1a** and was ruled out on energetic grounds. See the Supporting Information for details.
(25) BHLYP optimized geometries of annulenes typically show significant bond alternation, even for fairly delocalized systems. The GIAO-B3LYP/6-31G*//BHLYP/6-31G* NICS values of **1a,b** and **2a,b** reflect their various degrees of delocalization: **1a**, −12.5 ppm; **1b**, +1.5 ppm; **2a**, −12.4 ppm; **2b**, −14.0 ppm. The large negative NICS values for **1a** and **2a,b** yield the conclusion that these are strongly aromatic, whereas the negligible NICS value of **1b** indicates that it is nonaromatic.
(26) Δr here is defined as the difference, in Å, between the longest and shortest sp^2-sp^2 C−C bonds.
(27) (a) Anet, F. A. L. *J. Am. Chem. Soc.* **1962**, *84*, 671. (b) Hrovat, D. A.; Borden, W. T. *J. Am. Chem. Soc.* **1992**, *114*, 5879.
(28) Valley-ridge inflection points are well established, for example, in the ring opening of cyclopropylidene to allene and other systems: (a) Valtazones, P.; Elbert, S. T.; Ruedenberg, K. *J. Am. Chem. Soc.* **1986**, *108*, 3147. (b) Zhou, C.; Birney, D. M. *Org. Lett.* **2002**, *4*, 3279. (c) Singleton, D. A.; Hang, C.; Szymanski, M. J.; Meyer, M. P.; Leach, A. G.; Kuwata, K. T.; Chen, J. S.; Greer, A.; Foote, C. S.; Houk, K. N. *J. Am. Chem. Soc.* **2003**, *125*, 1319.
(29) Hong, Y. J.; Ponec, R.; Tantillo, D. J. *J. Phys. Chem. A* **2012**, *116*, 8902.